Spin-torque switching window, thermal stability, and material parameters of MgO tunnel junctions

T. Devolder,[1,a)] L. Bianchini,[1] K. Miura,[4] K. Ito,[4] Joo-Von Kim,[1] P. Crozat,[1] V. Morin,[1] A. Helmer,[1] C. Chappert,[1] S. Ikeda,[2,3] and H. Ohno[2,3]
[1]*Institut d'Electronique Fondamentale, Univ. Paris-Sud, 91405 Orsay, France and UMR 8622, CNRS, 91405 Orsay, France*
[2]*Center for Spintronics Integrated Systems, Tohoku University, 2-1-1 Katahira, Aoba- ku, Sendai 980-8577, Japan*
[3]*Laboratory for Nanoelectronics and Spintronics, Research Institute of Electrical Communication, Tohoku University, 2-1-1 Katahira, Aoba- ku, Sendai 980-8577, Japan*
[4]*Central Research Laboratory, Hitachi, Ltd., 1-280 Higashi-koigakubo, Kokubunji-shi, Tokyo 185-8601, Japan*

(Received 10 January 2011; accepted 22 March 2011; published online 18 April 2011)

We study the use of in-plane magnetized free layers with artificially lowered effective magnetization, in the context of spin-torque random access memories with magnetic tunnel junctions. We determine the field-voltage window for direct overwrite switching and thermal stability. We relate them to the magnetic constants extracted from the telegraph noise and high frequency noise exhibited by the junctions under specific conditions. © *2011 American Institute of Physics*. [doi:10.1063/1.3576937]

Spin torque[1,2] in magnetic tunnel junctions (MTJs) is considered as the viable option for allowing the scalability of magnetic random access memories (MRAMs). From a materials science point of view, the most mature systems are based on in-plane magnetized storage layers. For single free layers, there is a difficult tradeoff between lowering the switching current density and increasing the thermal stability[3] since both increase with the magnetization M_s. Indeed the stability is set by the energy barrier $\Delta E_0 = (1/2)\mu_0 M_S H_k V$ with V the cell volume and H_k the shape anisotropy field, which is proportional to M_s. At the same time, the average critical current density to switch the magnetization back and forth in the absence of thermal fluctuations is[4,5]

$$j_{C0} = (2e/\hbar)(\alpha t/P)\mu_0 M_s(H_x + H_k + M_{\mathrm{eff}}/2), \tag{1}$$

where P is the spin polarization, α and t are the free layer damping and thickness. The effective magnetization is $M_{\mathrm{eff}} = M_S - 2K/(\mu_0 M_S)$, where K is the out-of-plane anisotropy constant. A straightforward means to lower the j_{c0} without affecting the stability is to reduce M_{eff} through interface anisotropy, for instance by using[6] more Fe-rich CoFeB alloys on MgO, or by lowering the CoFeB thickness. This is the so-called "partial" perpendicular magnetic anisotropy concept.[7]

In this letter, we study MTJ elaborated following this concept, extracting each of the magnetic constants relevant in Eq. (1) in order to finally discuss scalability on this basis. For this we identify the writing window, i.e., the switching voltage and the field dependence thereof. We then measure the thermal stability factor by tuning down the energy barrier to artificially enhance thermal fluctuations and obtain H_k and M_s. We finally perform microwave noise spectroscopy to measure the spin wave frequencies, and model them to get M_{eff}, α and the exchange stiffness A.

[a)]Electronic mail: thibaut.devolder@u-psud.fr.

Our pillars are fabricated from stacks of composition cap/Ru/Ta/MgO (0.4)/$Co_{40}Fe_{40}B_{20}$ (2, free layer)/MgO (0.55, tunnel barrier)/$Co_{40}Fe_{40}B_{20}$ (3)/Ru(0.8)/$Co_{80}Fe_{20}$(2.5)/MnIr(8)/Py (1) /Ta/Ru/Ta/substrate, where thicknesses are in nanometer (Table I). A Ta-getter process was used before the deposition of the MgO layer in order to reduce the residual H_2O pressure to achieve low resistance-area (RA) products with high magnetoresistance.[8] As a result of Ta-getter, the base pressure reached levels below 10^{-9} Torr. The devices are rectangles with nominal dimensions of $L \times w = 200 \times 100$ nm^2 with (x) being the long axis parallel to the exchange biasing direction. In the parallel and antiparallel (AP) states, the junctions have typical resistances of 300 Ω and 500 Ω, respectively, corresponding to RA products of 6 and 10 Ω μm^2. Using Julliere's model[9] and assuming equal spin polarization P in the reference and free layers, we obtain $P \approx 70\%$ at zero bias and 56% at 500 mV. The free layer coercivity is 5 mT. Positive voltage corresponds to electrons passing from the free to the reference layer, favoring AP orientation. The switching thresholds are ±500 mV (current densities of −5 and 8×10^6 A/cm^2).

Let us first measure the switching voltage and its field dependence. We define the switching window as the coordinates in the $\{H_x, H_y, V\}$ parameter space, where the application of a voltage $\pm V$ and a field sets deterministically the state of the free layer. This is conveniently done by comparing the switching astroid recorded under positive and negative applied voltages (Fig. 1). Each astroid is compiled from a series of $R(H_x)$ loops recorded at fixed hard axis field H_y [cf. Fig. 1(a)], the used criteria being the field points H_{x0} maximizing $|dR/dH_x|$.

TABLE I. Magnetic properties of the $Co_{40}Fe_{40}B_{20}$ 2 nm thick free layer.

$\mu_0 M_S$ (T)	$\mu_0 M_{\mathrm{eff}}$ (T)	$\mu_0 H_K$ (mT)	A (pJ/m)	α
1.28 ± 0.15	0.45 ± 0.02	9 ± 1	23	0.014 ± 0.003

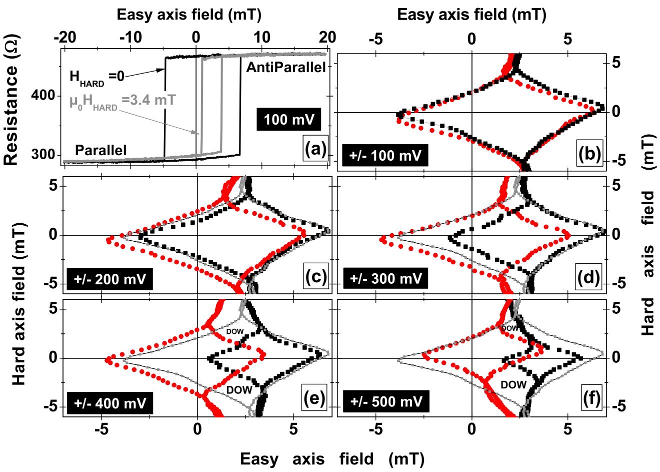

FIG. 1. (Color online) Quasistatic properties vs bias voltages. (a) Resistance vs easy axis field curves when a vanishing (black curve) or finite hard axis field is applied. [(b)–(f)] switching field astroids in constant positive (rectangles) or negative (circles) applied voltage. The gray astroids recall the 100 mV astroid. DOW stands for direct overwrite region.

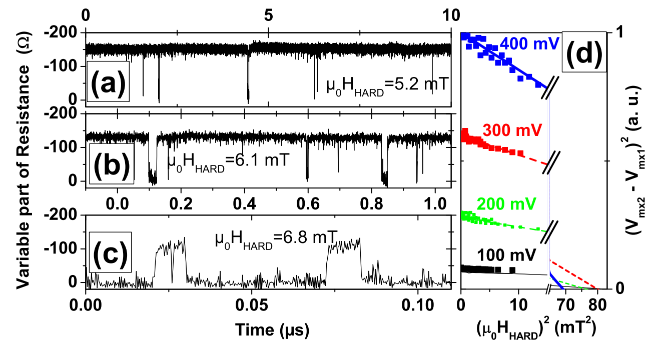

FIG. 2. (Color online) Resistance fluctuations under 400 mV for hard axis fields of (a) 5.2 mT, (b) 6.1 mT, and (c) 6.8 mT. Note that the timescale is reduced by 100 from panel (a) to (c). Panel (d) plot of the square of the difference of the voltages of the two metastable states vs the square of the hard axis field, and linear fits using Eq. (2) for various voltages.

At low bias [Fig. 1(b)], the astroid shape is consistent with the elongated shape of the device. Note however that the hard axis apex of the astroid is near 4 mT, i.e., *smaller* than the easy axis apex (coercivity, 5 mT), which would be impossible for a sample behaving like a thermally stable uniaxial macrospin.

The effect of moderate voltage (200 to 300 mV) is in line with expectations; it primarily reduces the coercivity of the transition favored by the voltage polarity. However, this coercivity is reduced for all values of hard axis field, in stark contrast to what happens in metallic spin-valves, where the spin torque is efficient only for fields oriented near the easy axis.[10]

At high voltages (400 and 500 mV), the positive voltage and negative voltage astroids are sufficiently separated that there exists two direct overwrite (DOW) zones, where the free layer is bistable in zero bias but writable and monostable in positive and negative voltages. The free layer can be effectively used as a memory when at least one of these region reaches zero field. Two unexpected points are worth noticing at ±500 mV. First, *all* coercivities are now reduced by the voltage whatever its polarity. Second, increasing the voltage does not systematically increase the surface of the DOW regions [compare the top DOW windows in Figs. 1(e) and 1(f)]. In all the devices we studied, the overlap between positive and negative voltage astroids ceases to exist for voltages scattered between ±450 and ±550 mV.

To understand this, we have extracted the material parameters of the free layer, starting by the shape anisotropy. Because of thermal fluctuations and departures from macrospin behavior, H_k can neither be extracted from the coercivity, nor from the hard axis apex of the astroids, which both significantly underestimate H_k. The misleading character of quasistatic astroids can be seen when recording time-resolved resistance traces in hard axis field conditions outside of the quasistatic astroid, i.e., for $H_y > 4$ mT and with near compensated easy axis applied fields. Under these conditions there are two degenerate stable states 1, 2 that exist and follow: $m_{y1,2} = H_y/H_k$ with $m_{z1,2} = 0$, $m_{x1} > 0$, and $m_{x2} < 0$. The two states have distinguishable resistances linearly linked to m_{x1} and m_{x2} with

$$(m_{x2} - m_{x1})^2 = 4[1 - (H_y/H_k)^2]. \tag{2}$$

The two states are separated by an energy barrier of $\Delta E = \Delta E_0 \times [1 - 2(H_y/H_k) + (H_y/H_k)^2]$ adjustable by the hard axis field. When $\Delta E \geq 21 k_B T$, the states are stable at a 1 s time scale and seen in our astroids. When the barrier is smaller, telegraph noise occurs and the system switches between m_{x1} and m_{x2} on a faster timescale, as evidenced in Fig. 2. Using Arrhenius modeling (not shown) the dwell times in Fig. 2 are consistent with $(\Delta E_0/k_B T) = 44.5 \pm 2.5$, ensuring nonvolatility.

A reliable way to obtain H_k is to plot the resistance difference at remanence in both the quasistatic loops and the telegraph noise data versus hard axis field. Linear fits through the Eq. (2) versus H_y^2 [Fig. 2(d)] yield the anisotropy field. At small and moderate voltage bias the fit yields $\mu_0 H_k = 8.9 \pm 0.7$ mT, almost twice greater than the hard axis apex of the astroid. At higher bias (400 mV) we get a smaller value 8.4 ± 0.7 mT, indicating either that the Oersted field distorts the remanent states or that there is a heating driven reduction in the magnetization. Taking the measured ΔE_0 and H_k, the magnetization of the free layer is estimated to be 1.28 ± 0.15 T, 20% less than the value measured before processing.

To measure M_{eff} and α, we have spectrally analyzed[11] the current noise passing through the MTJ at 100 mV. Several eigenmodes are sufficiently thermally populated to be detected as peaks in the spectra (Fig. 3). Modes of the synthetic antiferrimagnet reference layers, whose frequencies exhibit a minimum at the spin-flop transition near $H_x = +150$ mT, are not analyzed hereafter. Eigenmodes of the free layer appear as V-shape modes, with minima at the $\pm H_k$. Following Bayer *et al.*,[12] the eigenmode frequencies can be accounted for by assuming quantized wave vectors in the dispersion relations of spinwaves in the thin film limit with appropriate corrections for the dynamic demagnetizing tensors.[13] The overall slope of the modes' squared frequency versus field is a measure of M_{eff} while the mode-to-mode frequency spacing reflects the dynamic exchange field $(2A/\mu_0 M_S)[(n_L \pi/L^2) + (n_w \pi/w)^2]$, where n_L, n_w are the number of nodes in the free layer length and width. From fits of the lowest modes assumed to correspond to quasiuniform precessions, we get $\mu_0 M_{\mathrm{eff}} = 0.43 \pm 0.02$ T and $\mu_0 H_k = 10 \pm 2$ mT.

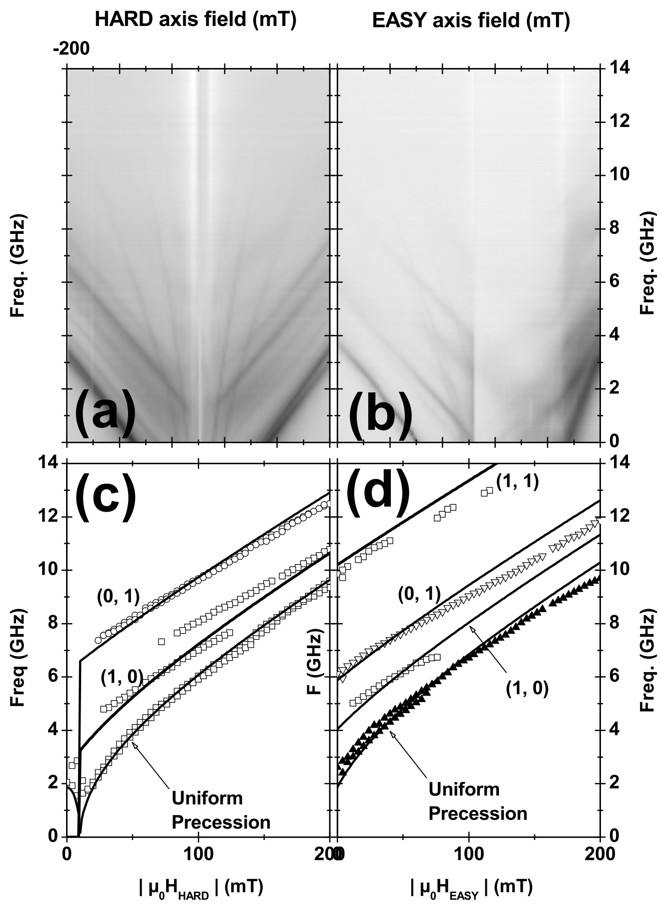

FIG. 3. High frequency current noise (log scale) spectroscopy under 100 mV dc for hard (a) and easy (c) axis fields. [(c) and (d)] Deduced spin wave frequencies and corresponding fits.

The full width at half maximum linewidth of the uniform mode is 350 ± 50 MHz at the largest field, consistent with an effective damping $\alpha_{\text{eff}}=[2\pi\Delta f/\gamma_0(M_{\text{eff}}+2H_k+2H_x)]=0.014\pm 0.003$. For the higher order spinwaves, a good fit of all dispersion curves with the nominal aspect ratio of 2 and a *uniform* M_S cannot be achieved. To account for the spacings between modes {0,0}, {1,0}, {0,1}, and {1,1}, an effective aspect ratio of 1.54 has to be chosen, which indicates a weaker dynamic dipolar pinning[12] at the longest edge of the device, whose origin is unclear but likely indicates weaker magnetism near the edge due to processing damage.[14] If we take the nominal length to be correct, one needs to assume a width $w=130$ nm. From the frequency of the length mode {1,0}, we deduce an exchange stiffness $A_{\text{CoFeB}}\approx 23$ pJ/m, which seems reasonable because it is between bulk iron (21) and bulk cobalt (28.5).

Let us compare our material data with the switching current density. Applying Eq. (1) with the bias dependence of P, we get $j_{C0}=3.4\times 10^6$ A/cm^2. This current is expected to be further reduced at 300 K by a factor $[1-(k_BT/\Delta E)\ln(\tau_p/\tau_0)]$, where $\tau_p\approx 0.01$ s is the experiment duration and $\tau_0^{-1}\approx 1$ GHz is an attempt frequency. This reduction factor is 0.64, which would yield $j_C(T=300\text{ K})\approx 2\times 10^6$ A/cm^2, i.e., twice lower than the experimental threshold. This difference deserves to be taken into account when evaluating the scaling potentials of MTJs.

In conclusion, further scaling of in-plane-magnetized-based MRAMs will require the damping to be reduced while relying on an additional source of thermal stabilization like an increased free layer thickness, if the RA product can reliably be decreased without sacrificing the tunnel magnetoresistance (TMR),[8] or like an exchange interaction with an antiferromagnet,[15] or a change to synthetic antiferromagnet free layer.[16]

T.D. acknowledges financial support from Hitachi, Ltd. This work was supported by the FIRST program from JSPS and the GCOE program at Tohoku University.

[1] J. C. Slonczewski, J. Magn. Magn. Mater. **159**, L1 (1996).
[2] L. Berger, Phys. Rev. B **54**, 9353 (1996).
[3] K. Yagami, A. A. Tulapurkar, A. Fukushima, and Y. Suzuki, J. Appl. Phys. **97**, 10C707 (2005).
[4] J. Z. Sun, Phys. Rev. B **62**, 570 (2000).
[5] J. A. Katine, F. J. Albert, R. A. Buhrman, E. B. Myers, and D. C. Ralph, Phys. Rev. Lett. **84**, 3149 (2000).
[6] S. Ikeda, K. Miura, H. Yamamoto, K. Mizunuma, H. D. Gan, M. Endo, S. Kanai, J. Hayakawa, F. Matsukura, and H. Ohno, Nature Mater. **9**, 721 (2010).
[7] J. Katine and E. E. Fullerton, J. Magn. Magn. Mater. **320**, 1217 (2008).
[8] Y. Nagamine, H. Maehara, K. Tsunekawa, D. D. Djayaprawira, N. Watanabe, S. Yuasa, and K. Ando, Appl. Phys. Lett. **89**, 162507 (2006).
[9] M. Julliere, Phys. Lett. A **54B**, 225 (1975).
[10] Y. Henry, S. Mangin, J. Cucchiara, J. A. Katine, and E. E. Fullerton, Phys. Rev. B **79**, 214422 (2009).
[11] T. Devolder, J. Hayakawa, K. Ito, H. Takahashi, S. Ikeda, P. Crozat, N. Zerounian, J.-V. Kim, C. Chappert, and H. Ohno, Phys. Rev. Lett. **100**, 057206 (2008).
[12] C. Bayer, J. Jorzick, B. Hillebrands, S. O. Demokritov, R. Kouba, R. Bozinoski, A. N. Slavin, K. Y. Guslienko, D. V. Berkov, N. L. Gorn, and M. P. Kostylev, Phys. Rev. B **72**, 064427 (2005).
[13] A. Helmer, S. Cornelissen, T. Devolder, J.-V. Kim, W. van Roy, L. Lagae, and C. Chappert, Phys. Rev. B **81**, 094416 (2010).
[14] S. Cornelissen, L. Bianchini, A. Helmer, T. Devolder, J.-V. Kim, M. O. de Beeck, W. V. Roy, L. Lagae, and C. Chappert, J. Appl. Phys. **105**, 07B903 (2009).
[15] I. L. Prejbeanu, M. Kerkes, R. C. Sousa, H. Sibuet, O. Redon, B. Dieny, and J. P. Nozières, J. Phys.: Condens. Matter **19**, 165218 (2007).
[16] J. Hayakawa, K. Ikeda, S. Miura, M. Yamanouchi, Y. M. Lee, R. Sasaki, M. Ichimura, K. Ito, T. Kawahara, R. Takemura, T. Meguro, F. Matsukura, H. Takahashi, H. Matsuoka, and H. Ohno, IEEE Trans. Magn. **44**, 1962 (2008).